molecular pharmaceutics

Article

pubs.acs.org/molecularpharmaceutics

Controlled Release Pulmonary Administration of Curcumin Using Swellable Biocompatible Microparticles

Ibrahim M. El-Sherbiny[†,‡] and Hugh D. C. Smyth*[,‡]

[†]Polymer Laboratory, Chemistry Department, Faculty of Science, Mansoura University, ET-35516 Mansoura, Egypt

[‡]Division of Pharmaceutics, College of Pharmacy, The University of Texas at Austin, Austin, Texas 78712, United States

ABSTRACT: This study involves a promising approach to achieve sustained pulmonary drug delivery. Dry powder particulate carriers were engineered to allow simultaneous aerosol lung delivery, evasion of macrophage uptake, and sustained drug release through a controlled polymeric architecture. Chitosan grafted with PEG was synthesized and characterized (FTIR, EA, DSC and 2D-XRD). Then, a series of respirable amphiphilic hydrogel microparticles were developed via spray drying of curcumin-loaded PLGA nanoparticles with chitosan-grafted-PEG or chitosan. The nanoparticles and microparticles were fully characterized using an array of physicochemical analytical methods including particle size, surface morphology, dynamic swelling, density, moisture content and biodegradation rates. The PLGA nanoparticles and the hydrogel microspheres encapsulating the curcumin-loaded PLGA nanoparticles showed average size of 221−243 nm and 3.1−3.9 μm, respectively. The developed carriers attained high swelling within a few minutes and showed low moisture content as dry powders (0.9−1.8%), desirable biodegradation rates, high drug loading (up to 97%), and good sustained release. An aerosolization study was conducted using a next generation impactor, and promising aerosolization characteristics were shown. *In vitro* macrophage uptake studies, cytotoxicity and *in vitro* TNF-α assays were performed for the investigated particles. These assays revealed promising biointeractions for the respirable/swellable nano−micro particles developed in this study as potential carriers for sustained pulmonary drug delivery.

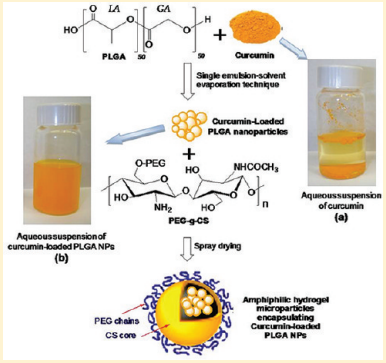

KEYWORDS: *nanoparticles, microspheres, PLGA, chitosan, PEG, curcumin, pulmonary, sustained, lung, drug delivery*

1. INTRODUCTION

A significant body of research has recently focused on pulmonary drug delivery as an attractive route for the administration of a wide range of therapeutics and for the ever-expanding array of local and systemic diseases.[1−4] However, the efficient clearance of exogenous substances including delivered drugs from the deep lung through either rapid drug absorption or macrophage uptake in the alveolar region has hindered successful development of carrier systems suitable for sustained pulmonary drug delivery. Various approaches have been reported in the literature to overcome these shortcomings. These include the use of conjugated and PEGylated drugs,[5,6] microencapsulated polymer particles,[7−9] nanoparticles,[10−12] large porous particles,[13−16] and swellable microparticle/nano−microparticle systems being developed by our group.[17−19]

The major challenge in this area of inhalation therapy is that the most appropriate aerodynamic size range for particles to be respirable (0.5−5 μm) is also considered the optimum size for the rapid uptake by the macrophages in the alveolar region. This leads to a rapid phagocytosis of carrier particles and loss of the therapeutic molecules. Although the phagocytosis, which may be accompanied by release of the therapeutic molecules within the macrophages (macrophage targeting), is sometimes favorable, such as in the case of tuberculosis, this rapid phagocytosis process represents a major obstacle toward sustained drug release in the lung for most therapeutic agents. Therefore, the strategy suggested in this study for sustained controlled pulmonary drug delivery involves the engineering of dried hydrogel delivery carrier systems that are able to provide respirable aerodynamic size, and offer stealth characteristics to hide themselves from macrophages in addition to showing desirable controlled release kinetics. Our earlier studies[17−19] showed that hydrogel microparticles of appropriate aerodynamic diameters can be delivered as dry powders with a high respirability. These microparticles attained relatively large swelled sizes in moist conditions such as lungs within a few minutes. The large swelled sizes enabled the particles to evade macrophage uptake and consequently be able to confer sustained drug release.

Curcumin, a yellow substance from *Curcuma longa*, has been selected in this study as a target therapeutic molecule, due to its wide range of superior pharmaceutical applications. Curcumin is a pharmacologically safe compound and it has been used for centuries as a dietary spice and a food-coloring material, at relatively high doses up to 100 mg/day.[20] Some clinical trials have illustrated that high doses of curcumin up to 8 g/day when

Received: July 11, 2011
Revised: November 26, 2011
Accepted: December 2, 2011
Published: December 3, 2011

taken by mouth for 3 months are acceptable.[21] A number of *in vitro* and *in vivo* studies have also revealed good anti-inflammatory and antioxidant characteristics of curcumin.[22,23] Curcumin also showed a potential for inhibition of tumorigenesis[24] and correction of cystic fibrosis imperfections.[25] In addition, curcumin has been found promising in the treatment of asthma and chronic obstructive pulmonary diseases.[26]

In spite of these various promising therapeutic applications of curcumin, its therapeutic efficacy is limited due to its very poor water solubility and consequently very low systemic concentrations when consumed orally. In addition, curcumin suffers from chemical instability in the gastrointestinal tract. Phase 1 and 2 trials have shown rapid clearance of curcumin from the body and a very limited average peak serum concentration (1.77 ± 1.87 μM per a dose of 8 g).[21,27] Enhanced targeting and delivery of curcumin can increase local concentrations, and the sustained release can improve the therapeutic potential of this therapeutic molecule. In addition, pulmonary administration of sustained release formulations of curcumin using dry powder inhalers (DPIs) would enable delivery of locally high doses of curcumin to the lung epithelia for the treatment of various pulmonary defects and diseases.[28]

This study involves the development of a new carrier system for controlling pulmonary delivery of curcumin. This carrier system combines the advantages of the respirable/swellable hydrogel microspheres proposed in our earlier studies[17−19] in addition to drug loaded nanoparticles. Nanoparticles have shown an obstinate residency in the lungs as reported by Oberdorster[29] with the ability to evade phagocytosis and mucociliary clearance.[30−32] Here, we describe the incorporation of drug-loaded nanoparticles into swellable/respirable microparticles, as a strategy for attaining a sustained drug release, not only in the alveolar region where macrophage clearance predominates but potentially throughout the lumen of the lungs. Furthermore, encapsulation of drug-loaded nanoparticles into microparticles for pulmonary drug delivery allows for efficient deposition in the airways and avoidance of exhalation of the nanoparticles from the lungs following inspiration.[33]

The developed carrier system composed of curcumin-loaded poly(D,L-lactic-*co*-glycolic acid) (PLGA) nanoparticles encapsulated in amphiphilic hydrogel microspheres based on PEG-chitosan (Cs) graft copolymer. PLGA, a copolymer of lactic acid (LA) and glycolic acid (GA), has been selected due to its various characteristics such as biodegradability, biocompatibility, and very minimal systemic toxicity as the body deals efficiently with its hydrolysis end products, LA and GA.[34] Cs also has numerous desirable properties including biodegradability, biocompatibility, and nontoxicity[35] in addition to its significant role in improving the drug absorption in lung tissues due to the Cs transient effect in opening the intercellular tight junction of the pulmonary epithelium.[36] Grafting of the biocompatible PEG onto the Cs backbone was carried out for further enhancement of the Cs physicochemical properties and to offer stealth characteristics for the developed microparticles to evade the macrophage uptake.

2. MATERIALS AND METHODS

2.1. Materials. *2.1.1. Chemicals.* Chitosan (average M_w, 354 kDa, as determined using viscometry methods in a solvent of 0.1 M acetic acid/0.2 M NaCl maintained at 25 °C; % N-deacetylation, 76.4%, as determined by FTIR spectroscopy and elemental analysis), monomethoxy-poly(ethylene glycol) (m-PEG, M_n 5 kDa), succinic anhydride and 1-hydroxybenzotrizole (HOBt) were supplied by Aldrich (St. Louis, MO). 1-Ethyl-3-(3-dimethylaminopropyl)carbodiimide hydrochloride (EDC·HCl) was obtained from Fluka Chemical Corp. (Milwaukee, WI). Curcumin and 4-dimethylaminopyridine (DMAP) were provided by Sigma (St. Louis, MO). Poly(D,L-lactic-*co*-glycolic acid) (PLGA) copolymer (50/50 molar composition of lactic/glycolic acids and inherent viscosity of 0.15−0.25 dL/g), polyvinyl alcohol, PVA (MW 12−23 kDa, 87−89% hydrolyzed), phthalic anhydride, dioxane, triethylamine and dimethylformamide (DMF) were obtained from Sigma-Aldrich (St. Louis, MO). Methylene chloride was purchased from Fisher Scientific (Fairlawn, NJ). Absolute ethanol, phosphate buffer saline (PBS pH 7.4) and all other reagents were of analytical grade and used as received.

2.1.2. Cell Culture. The mouse macrophage (*Mus musculus*) cell line, RAW 264.7 (8.8×10^5 total cells/mL) with viability of 82.6−91.2% was provided by American Type Culture Collection, ATCC (Manassass, VA). Fetal bovine serum (FBS) was obtained from ATCC. The growth medium, Dulbecco's modified Eagle medium (DMEM), was purchased from Gibco, Invitrogen, Grand Island, NY. One micrometer polystyrene (PS) beads (Fluospheres fluorescent (505/515) were obtained from Invitrogen Eugene, OR, and the 112 μm PS particles were purchased from Bangs Laboratories, Inc., Fishers, IN. The paraformaldehyde (PFA) 4% solution in PBS was provided by USB Corporation, Cleveland, Ohio.

2.2. Methods. *2.2.1. Preparation of PEG/Cs Graft Copolymer.* The copolymer of PEG grafted onto Cs was prepared by a method reported in our earlier study[18] and described briefly as follows:

(a) Conversion of m-PEG into m-PEG-COOH: m-PEG (100 g, 20 mmol), DMAP (2.44 g, 20 mmol), succinic anhydride (2.4 g, 24 mmol) and triethylamine (2.02 g, 20 mmol) were dissolved in 350 mL of dry dioxane. The mixture was stirred at room temperature for 48 h under a dry nitrogen atmosphere. Dioxane was then evaporated using a rotary evaporator, and the residue was taken up in CCl_4, filtered and precipitated by diethyl ether to produce a white powder of m-PEG-COOH.

(b) N-phthaloylation of Cs: phthalic anhydride (44.8 g, 5 molar equiv to pyranose rings) was reacted with 10 g of Cs in 200 mL of DMF at 130 °C under dry nitrogen atmosphere for 8 h. The resulting *N*-phthaloyl Cs (NPHCs) was then collected by filtration after precipitation in ice−water, washed with methanol and then dried under vacuum at 40 °C to give a pale brown product (NPHCs).

(c) Grafting of m-PEG-COOH onto NPHCs: m-PEG-COOH (37.9 g) was stirred with NPHCs (5.0 g, 0.4 molar equiv to m-PEG-COOH) in 75 mL of DMF. Afterward, HOBt (3.4 g, 3 molar equiv to m-PEG-COOH) was added, as a catalyst, with stirring at room temperature until obtaining a clear solution. The EDC·HCl (4.25 g, 3 molar equiv to m-PEG-COOH) was then added, and the mixture was stirred overnight at room temperature. A purified PEG-*g*-NPHCs copolymer (5.47 g, white product) was obtained after dialysis of the reaction mixture against distilled water and washing with ethanol. The grafting percentage (*G*%) of PEG-*g*-NPHCs was determined gravimetrically using the following relationship:

$$G\% = [(Wc - W_0)/W_0] \times 100 \quad (1)$$

where W_c and W_0 are the weights of PEG-*g*-NPHCs and NPHCs, respectively.

Table 1. Composition and Some Characteristics of the Prepared Hydrogel Microspheres Encapsulating Curcumin-Loaded PLGA Nanoparticles

sample code	PLGA nanoparticles: mg	PLGA nanoparticles: *W*%	PEG-*g*-CS (mg)	CS (mg)	moisture content (%)	EE %[a] ± SD	tapped density (g/mL)	VMD[b] (μm)	span[c]	d_a[d]
NMP1	175	35	500		1.36 ± 0.21		0.190	3.11 ± 0.02	2.01 ± 0.06	1.36 ± 0.05
NMP2	250	50	500		1.46 ± 0.06		0.165	3.57 ± 0.01	1.71 ± 0.03	1.45 ± 0.04
NMP3	375	75	500		1.22 ± 0.12		0.137	3.62 ± 0.04	1.31 ± 0.07	1.34 ± 0.01
NMP4	175	35		500	1.41 ± 0.25		0.192	3.34 ± 0.06	1.23 ± 0.04	1.46 ± 0.03
NMP5	250	50		500	1.39 ± 0.07		0.160	3.46 ± 0.02	1.09 ± 0.00	1.38 ± 0.02
NMP6	375	75		500	0.90 ± 0.31		0.176	3.91 ± 0.10	1.35 ± 0.10	1.64 ± 0.04
NMP1-Cur	175	35	500		1.21 ± 0.10	89.63 ± 1.28	0.149	3.08 ± 0.04	1.75 ± 0.07	1.19 ± 0.01
NMP2-Cur	250	50	500		1.37 ± 0.18	94.42 ± 1.71	0.146	3.17 ± 0.03	2.11 ± 0.03	1.21 ± 0.03
NMP3-Cur	375	75	500		1.76 ± 0.14	93.35 ± 3.01	0.098	3.50 ± 0.46	1.63 ± 0.06	1.09 ± 0.02
NMP5-Cur	250	50		500	1.54 ± 0.09	93.00 ± 1.32	0.209	3.94 ± 0.01	1.89 ± 0.08	1.80 ± 0.01

[a]EE %: entrapment efficiency %. [b]Volume mean diameter, VMD. [c]Span = $(D_{90} - D_{10})/D_{50}$. [d]d_a, aerodynamic diameter.

(d) Conversion of PEG-*g*-NPHCs into PEG-*g*-Cs: Briefly, PEG-*g*-NPHCs (4.0 g) was heated to 100 °C with stirring under nitrogen in 15 mL of DMF. Then 20 mL of hydrazine monohydrate was added, and the reaction was continued for 2 h. The resulting PEG-*g*-Cs copolymer was extensively purified via dialysis against a mixture of deionized water and ethanol (1:1) and then dried under vacuum at 40 °C. The average M_w of the obtained PEG-*g*-Cs copolymer was determined using viscometry methods in a solvent of 0.1 M acetic acid/0.2 M NaCl maintained at 25 °C.

2.2.2. Characterization. The FTIR spectra of m-PEG-COOH, NPHCs, PEG-*g*-NPHCs and PEG-*g*-Cs was recorded using a Nicolet 6700 FTIR spectrometer, and the elemental analysis was carried out using a Costech ECS4010 elemental analyzer coupled to a Thermo-Finnigan Delta Plus isotope ratio mass spectrometer. The crystallography patterns of the powder polymer samples were examined by X-ray diffraction (XRD) in a reflection mode with the aid of a Scintag Pad V diffractometer with Data-Scan 4 software (MDI, Inc.) for data collection and system automation. Cu Kα radiation (40 kV, 35 mA) was employed with a Bicron Scintillation detector (with a pyrolitic graphite curved crystal monochromator). The data were analyzed with Jade Software (Ver 9.0 from MDI, Inc.). Samples were run at 2θ values of 5° to 45° at a continuous scan/data collection rate of 0.5 deg min^{-1}. Differential scanning calorimetry (DSC) was carried out using a DSC 2920 (Modulated DSC, TA Instruments) in a nitrogen atmosphere with a temperature range of −40 to 400 °C at a heating rate of 10 °C min^{-1}. Preweighed samples (10−15 mg) were placed in aluminum sample pans and sealed. An empty aluminum pan of approximately equal weight was used as a reference. All peaks were recorded, and the areas under peaks were converted into enthalpy values.

2.2.3. Preparation of Curcumin-Loaded PLGA Nanoparticles. The curcumin-loaded PLGA nanoparticles were prepared using the "single emulsion−solvent evaporation method" through a modified procedure to that described in the literature.[37] Briefly, 500 mg of PLGA was dissolved in 10 mL of methylene chloride. A solution of 100 mg of curcumin dissolved in 10 mL of ethanol was added with stirring to the PLGA solution. Afterward, the PLGA/curcumin mixture was added dropwise with high vortexing to a surfactant solution (25 mL of 3% w/v aqueous PVA solution). Once all of the PLGA/curcumin mixture was added, the contents were sonicated for 2 min at 60% amplitude with a probe type sonicator (Misonix ultrasonic processor, S-4000, Misonix Inc., CT, USA) to create an oil-in-water emulsion. The sonication step was repeated three times until the desired size was obtained. The sonication process was carried out in an ice−water bath with using pulse function (pulse on 5 s and pulse off 5 s) to prevent heat buildup of the PLGA/curcumin solution during the sonication. After sonication, the emulsion was immediately poured into 100 mL of 0.5% w/v aqueous PVA solution under rapid stirring. The resulting nanosized PLGA emulsion was then stirred overnight in a fume hood in an uncovered beaker to allow for ethanol and methylene chloride evaporation. The produced PLGA nanoparticle suspension was diluted to 150 mL volume with deionized water and further employed in the preparation of the swellable hydrogel microspheres.

2.2.4. Preparation of the Respirable/Swellable Microspheres Encapsulating Curcumin-Loaded PLGA Nanoparticles. Respirable/swellable hydrogel microspheres were developed via spray drying of a homogeneous mixture of the curcumin-loaded PLGA nanoparticles with either PEG-*g*-Cs copolymer or Cs. Typically, predetermined volumes (Table 1) of the 0.33% w/v curcumin-loaded PLGA nanoparticle suspension obtained in the previous section was added dropwise with homogenization (10,000 rpm) to 100 mL of 0.5% w/v of either PEG-*g*-Cs or Cs solution (dissolved in 0.06% acetic acid). Then, the homogenized polymer mixtures were spray-dried with a 0.7 mm two-fluid pressurized atomizer at a feed rate of 25% (6 mL/min) in a Büchi Mini spray dryer B-290 (Büchi, Switzerland). The flow rate of atomizing air was 500−600 NL/h with inlet temperature adjusted at 125 °C, and the outlet temperature varied between 65 and 68 °C. The obtained hydrogel powder was collected, and the yield (%) of the spray drying process was calculated.

The entrapment efficiency (EE%) of curcumin was determined by dissolving dried plain and curcumin−loaded hydrogel microspheres in sodium acetate buffer, pH 3.4 to make about 5 mg/mL solutions. The buffer solution has been prepared by mixing 5 volumes of 0.1 M sodium acetate with 95 volumes of 0.1 M acetic acid. Then, absorbance of the solutions was measured, after dilution with the same volume of ethanol, at 430 nm by UV−vis spectrophotometry (Infinite M 200 fluorophotometer, TECAN, USA). The amount of loaded

curcumin per gram of microspheres was then calculated with the aid of a standard curve of curcumin in sodium acetate buffer (pH 3.4)/ethanol (1:1) vs absorbance. The solution of microspheres encapsulating plain PLGA nanoparticles was used as absorbance background control. It has been found in prior studies that there was no absorbance interference from the plain microspheres under the same conditions. The mean values from three replicates ± SD were obtained. The entrapment efficiency (EE %) of the curcumin was calculated according to the following relationship:

$$\text{EE}\,\% = \left(\frac{m_r}{m_i}\right) \times 100 \tag{2}$$

where m_i and m_r are the amounts (mg) of the curcumin initially loaded and remaining in the microspheres, respectively.

2.2.5. Determination of Particle Size. The size of the prepared curcumin-free and curcumin-loaded PLGA nanoparticles was estimated at λ_{max} of 500 nm using dynamic light scattering, DLS (Wyatt Technology Corporation Dyna Protitan DLS), with a refractive index of 1.363 for the solvent. The volume median diameters (VMD, μm) of developed hydrogel microspheres encapsulating PLGA nanoparticles and the particle size distributions were measured using laser diffraction (SYMPATEC, Sympatec Gmbt, System Partikl-Technik, Germany with a He−Ne laser beam 5 mW max at 632.8 nm) with the aid of WINDOX 5.1.2 software. The measurements were performed in the range 0.5−175 μm for the suspension of the hydrogel microspheres in acetone. Acetone was used as a dispersion solvent to avoid the swelling of the particles during the size measurements. The particle densities were also approximated from tapped density measurements, and then the aerodynamic diameters of the hydrogel microspheres were determined using the following relationship:

$$d_a = d_g(\rho_p/\rho_0\chi)^{0.5} \tag{3}$$

where, d_a and d_g are the aerodynamic and geometric (VMD) diameters (μm), ρ_p is the microsphere density (g/mL), ρ_0 is the standard density (1 g/mL) and χ is the dynamic shape factor (χ =1 in case of spherical particles).

2.2.6. In vitro aerosolization study. A dry powder aerosolization study was performed *in vitro* for the NMP1 hydrogel microspheres encapsulating curcumin-loaded PLGA nanoparticles, as example, using a Next Generation Impactor (NGI, MSP Corporation, MN). Typically, a size 3CS capsule (Capsugel, MA) was filled with 10−15 mg of the microsphere powder. The capsule was placed in a hand-held, dry-powder inhaler (Handihaler) and was punctured prior to inhalation. Then, a pump (Copley HCP5, Nottingham, U.K.) was actuated to simulate an inspiration process at air flow rate of 60 ± 5% L·min^{-1} for a duration of 6 s. The aerosolization process was performed in triplicate with one capsule used in each run. The powder emitted from the capsule in each run was deposited on different stages of the NGI. Each stage contained a predetermined volume (5−15 mL) of sodium acetate buffer, pH 3.4 as a collecting solvent. In addition, the hydrogel powders deposited on the inhaler, capsule and the adapter were collected in appropriate volumes of the collecting solvent. The amount of curcumin-loaded powder collected in each stage was then determined spectrophotometrically (Infinite M 200 fluorophotometer, TECAN, USA), after dilution with an equal volume of ethanol, at 430 nm. The analysis of powder deposition in the inhaler, capsule, adapter, throat and NGI stages allowed the determination of different deposition parameters such as the emitted fraction (E_F%, the percent of total loaded powder mass exiting the capsule), respirable fraction (R_F%) and the fine particle fraction (FP_F%) according to the following relationships:

$$E_F\% = \frac{m_{full} - m_{empty}}{m_{powder}} \times 100$$

$$R_F\% = \frac{m(d_a < 4.46\,\mu\text{m})}{m_t} \times 100$$

$$FP_{F<4.46\,\mu m}\% = \frac{m(d_a < 4.46\,\mu\text{m})}{m_{NGI+throat+adapter}} \times 100 \tag{4}$$

where m_{full} and m_{empty} are the weights (mg) of capsule before and after simulating inhalation and m_{powder} is the initial weight (mg) of the curcumin-loaded powder in the capsule. $m(d_a <$ 4.46 μm), m_t and $m_{NGI+throat+adapter}$ are the amount of particles with aerodynamic diameters less than 4.46 μm, total amount of particles and the summation of particle amounts collected from NGI stages, throat and adapter, respectively. The mass median aerodynamic diameters (MMAD, μm) of the aerosolized hydrogel particles were also estimated experimentally from the analysis (using the Web-based application, MMAD Calculator) of the deposition of curcumin-loaded hydrogel particles in the different NGI stages.

2.2.7. Surface Morphology. The morphology of the developed hydrogel microspheres was investigated by SEM (Zeiss supra 40 VP scanning electron microscope). Dry microspheres were mounted on aluminum stubs with double-sided conducting carbon tapes and coated with a 50/50 mixture of Pt/Pd to minimize surface charging. The samples were scanned at an accelerating voltage of 20 kV. The surface morphology of the hydrogel microspheres encapsulating PLGA nanoparticles was also examined using atomic force microscopy, AFM (Multi-Mode scanning probe atomic force microscope, Veeco Instruments, USA).

2.2.8. Determination of Moisture Contents. The moisture contents of the prepared microspheres encapsulating PLGA nanoparticles were measured with the aid of a HR83 Halogen Moisture Analyzer (Mettler-Toledo GmbH, Switzerland). Samples of approximately 150−200 mg were tested at a drying temperature of 120 °C for 2 min. The moisture contents were obtained as the weight loss (%) and calculated as the average ± SD from three independent measurements.

2.2.9. Dynamic Swelling Study. The swelling characteristics of the hydrogel microspheres in PBS (pH 7.4) were investigated by determining the increase in both medium diameter (X_{50}, μm) and the volume median diameter (VMD, μm) of microspheres with time with the aid of a laser diffractometer (SYMPATEC, Sympatec Gmbt, System Partikl-Technik, Germany).

2.2.10. In Vitro Enzymatic Degradation Study. An *in vitro* enzymatic degradation study of the hydrogel microspheres was performed in the presence of lysozyme (2 mg/mL PBS, pH 7.4) according to the protocol described by Hirano et al.[38] Predetermined weights of hydrogel microspheres (10−20 mg) were transferred to microcentrifuge tubes and incubated with 1.0 mL of lysozyme solution at 37 °C in a shaking (100 rpm) incubator (VWR incubating orbital shaker, VWR International, Brisbane, CA, USA) for 1 h until microspheres almost attained

Scheme 1. Synthesis of the PEG-Cs Graft Copolymer

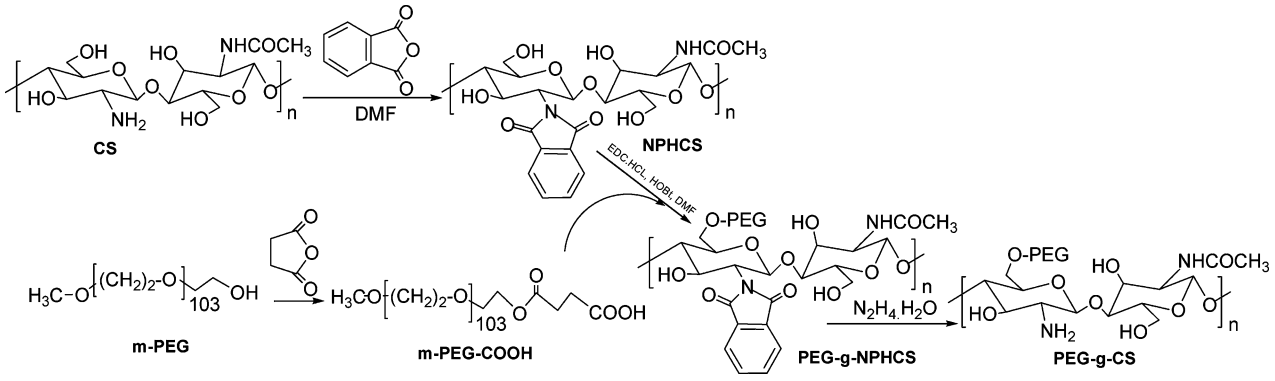

equilibrium swelling. The samples were then centrifuged for 2 min at a speed of 15000 rpm, and the weights of swollen hydrogel microspheres (W_s) were determined after discarding the supernatant. Afterward, a fresh lysozyme solution (1 mL) was added to the swollen particles. At intervals, starting from determination of W_s, the steps of centrifugation and weighing were repeated and the final weights (W_t) of microspheres at these intervals were determined. The percent weight remaining (W_r%) of the samples due to enzymatic degradation were calculated according to the following relationship:

$$W_r\ (\%) = 100 - \left(\frac{(W_s - W_t)}{W_s} \times 100 \right) \quad (5)$$

where W_s and W_t are the weights of sample after 1 h swelling in lysozyme solution and after incubation with lysozyme for a given time, t, respectively.

2.2.11. In Vitro Curcumin Release Studies. The *in vitro* release profiles of curcumin from the hydrogel particles were determined by transferring certain amounts (20−30 mg) of curcumin-loaded microspheres to scintillation vials containing 15 mL of PBS, pH 7.4. The samples were then maintained at 37 °C in a shaking (100 rpm) incubator (VWR incubating orbital shaker, VWR International, Brisbane, CA, USA). At intervals, 50 μL aliquots were withdrawn and diluted with equal volumes of ethanol and then analyzed spectrophotometrically at λ_{max} 430 nm using Infinite M 200 fluorophotometer, TECAN, USA. The withdrawn aliquots were replaced with equal volumes of fresh PBS, 7.4 buffer, to keep the volume of release medium constant. The amounts of curcumin released (μg) from hydrogel microspheres were calculated with the aid of a standard curve of curcumin in PBS, pH 7.4/ethanol (1:1). The results were calculated in terms of cumulative release (%, w/w) relative to the actual entrapped weight of curcumin in the hydrogel microspheres. The collected data represent mean ± SD from three independent release experiments.

2.2.12. Cytotoxicity Assay. To assay the effect of the developed hydrogel microspheres encapsulating PLGA nanoparticles on the viability, RAW 264.7 cells were seeded in 96-well plates at 50,000 cells/well and incubated for 24 h at 37 °C and 5% CO_2. Fifty microliters of various concentrations (320, 800, and 1600 μg/mL) of the hydrogel microspheres was added into the culture medium of the plate and incubated for 24 h. Control cells were grown without adding hydrogel microspheres. The cell viability was estimated using a MTT cell proliferation assay kit provided by American Type Culture Collection, ATCC (Manassas, VA). After addition of the MTT reagent (10 μL), the cells were incubated at 37 °C and 5% CO_2 for 4 h until the purple precipitate was visible. Then, 100 μL of the detergent reagent was added and the cells were left at room temperature in the dark for 2 h. The cell viability was then estimated by recording absorbance at 570 nm. Data were expressed as mean absorbance value (OD) of triplicate samples plus standard deviation of the mean.

2.2.13. Tumor Necrosis Factor Alpha (TNF-α) Assay. The TNF-α was quantified in the RAW 264.7 cells containing swellable particles and controls using a Mouse TNF-α ELISA kit (Thermo Scientific, Rockford, IL) according to the manufacturer's instructions.

2.2.14. Macrophage Uptake Study. Raw 264.7 macrophage cells (ATCC TIB-71; Manassass, VA) were seeded at about 50,000 cells/well into a 24-well plate (Falcon 353047 Multiwell; Franklin Lakes, NJ). The medium, DMEM, was removed after 24 h of incubation, and the cells were washed with PBS, pH 7.4. Then, 25 μL of DMEM containing control particles (either 1 or 112 μm PS particles) was added to predetermined wells. Curcumin-loaded swellable particles suspended in 25 μL of DMEM were also added to the labeled wells.[18] The microparticles (PS and swellable particles) were added at desired concentrations so that almost equal numbers of each particle type were incubated with the cells (about 10^5 particles/well). A number of wells were left without addition of any particles as cell controls. After each time point (30 min, 2 and 24 h), the medium was removed and the cells were washed twice with PBS, fixed with 0.5 mL of 4% PFA solution for 10 min and then washed with PBS to remove any residual PFA. The particle uptake by macrophages was quantified by measuring the absorbance at 430 nm corresponding to the uptaken fluorescent particles after washing the excess particles. The wells were then imaged with the aid of an inverted Leica fluorescent microscope at 10× and 20× magnifications.

2.2.15. Statistical Analysis. The obtained data was analyzed and expressed as mean ± SD. The effect of various parameters on the characteristics of the prepared PLGA nanoparticles/hydrogel microspheres were statistically analyzed by one-way ANOVA using Excel (Microsoft Office 2007). Differences were considered significant at the level of $p < 0.05$.

3. RESULTS AND DISCUSSION

3.1. Synthesis of PEG/Cs Graft Copolymer. A biodegradable copolymer of m-PEG grafted onto the Cs backbone was prepared through a modified method reported in our earlier study.[18] The copolymer synthesis was achieved through a systematic series of reactions (Scheme 1) starting with protection of the NH_2 groups of Cs via a phthaloylation

Table 2. Elemental Analysis and FTIR Data of the Synthesized Compounds

compound	EA (%)	FT-IR (ν_{max}, cm^{-1})
m-PEG-COOH ($C_{231}H_{460}O_{117}$)	anal. calcd (%), C 54.35, H 9.02; found (%), C 56.8, H 9.19	3496, 2882, 1733, 1102
N-PHCs $(C_8H_{13}NO_5)_{0.2363}(C_6H_{11}NO_4)_{0.016}(C_{14}H_{13}NO_6)_{0.747}$	anal. calcd (DS = 0.98) (%), C 55.74, H 4.84, N 5.23; found (%), C 60.31, H 4.83, N 4.92	3281, 2961, 1775, 1698, 1395, 1058, 732
PEG-*g*-NPHCs	found (%), C 56.16, H 4.69, N 5.15	3423, 2879, 1736, 1703, 1096, 723
PEG-*g*-Cs	found (%), C 40.46, H 4.71, N 14.44	3312, 2879, 1708, 1096

process to produce phthaloyl Cs (NPHCs). The FTIR of NPHCs (Table 2) showed absorbance signals at 1395 and 732 cm^{-1} which can be assigned for the "aromatic C═C" and "aromatic C−H" bonds of the phthaloyl groups, respectively. The substitution degree (DS) of phthaloyl groups was estimated at 0.97 using elemental analysis. The m-PEG was modified into carboxyl-capped m-PEG precursor (m-PEG-COOH) through reaction with succinic anhydride. The synthesis of m-PEG-COOH was confirmed with the aid of FTIR and EA. Grafting of m-PEG-COOH onto NPHCs backbones was then achieved (*G*%: 9.3%). The PEG/Cs graft copolymer (with average M_w of 472 kDa, as determined using viscometry methods) was obtained by demasking of the NH_2 groups of PEG-*g*-NPHCs copolymer using hydrazine monohydrate. The synthesis of PEG-*g*-Cs was also confirmed using EA and FTIR (Table 2). The synthesis steps of the graft copolymer are demonstrated in Scheme 1.

The synthesis of the PEG-*g*-Cs copolymer was also confirmed by studying its thermal behavior as compared to the starting materials, PEG-COOH and Cs as shown in Figure

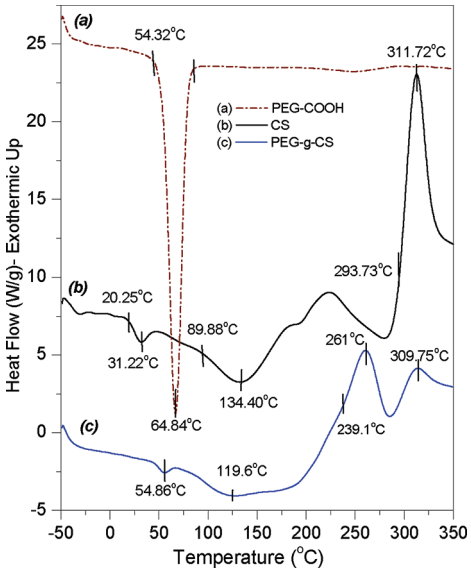

Figure 1. DSC characterizations of the starting materials: (a) PEG-COOH and (b) Cs in comparison to (c) the prepared PEG-*g*-Cs copolymer.

1. The DSC thermogram of PEG-COOH (Figure 1a) revealed an endothermic peak at about 65 °C which corresponds to its melting process. In the case of the Cs thermogram (Figure 1b), an endothermic peak started at about 90 °C which was ascribed to the loss of bound water. Cs also showed an exothermic peak at 312 °C which may correspond the decomposition of glucosamine units.[40,41] The thermogram of the synthesized PEG-*g*-Cs copolymer (Figure 1c) illustrated an endothermic peak at 55 °C which can be related to the melting of the grafted PEG side chains. Also, an endothermic peak was observed at 119 °C which was attributed to the loss of bound water. The exotherm appeared at 310 °C may be ascribed to the thermal decomposition of the copolymer.

Figure 2 depicts the XRD patterns of the synthesized graft copolymers (PEG-*g*-NPHCs and PEG-*g*-Cs) as compared to

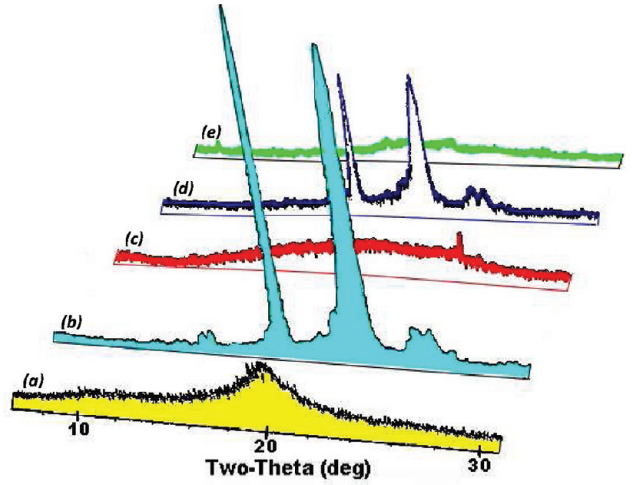

Figure 2. The XRD patterns of (a) CS, (b) m-PEG-COOH, (c) NPHCS and (d) PEG-*g*-NPHCS and (e) PEG-*g*-CS copolymer.

the other polymers (Cs, NPHCs and PEG-COOH). As apparent from Figure 2, the Cs is mainly amorphous with a very marked broad band centered at 2θ of 20°. This band may be attributed to the amorphous glassy structure of the Cs. The diffractogram of Cs also showed a relatively weak inflection point in the pattern at a 2θ value of about 11°. The diffractogram of NPHCs also revealed an amorphous nature with a broad hump over a range of 19° and centered at 2θ of 23°. Both diffractograms of m-PEG-COOH and PEG-*g*-NPHCs, however, illustrated a development of very similar crystalline profiles with a greater peak intensity and indicative of more crystalline nature in the case of m-PEG-COOH. The prepared PEG-*g*-Cs copolymer was found to be typically amorphous with the appearance of some small peaks barely above the background levels. From the obtained XRD patterns, it seems that the phthaloylation of Cs kept the amorphous nature of Cs chains in the obtained NPHCs. However, it appears that grafting of equal side chains of PEG onto the NPHCs backbones has assisted in a certain way in well ordering the polymeric chains toward a more crystalline diffraction pattern in the resulting PEG-*g*-NPHCs. In the case of PEG-*g*-Cs copolymer, the elimination of the phthaloyl groups from the NPHCs-*g*-PEG backbones led to a kind of destruction in chain ordering which turned the resulting PEG-*g*-Cs into a more amorphous material.

dx.doi.org/10.1021/mp200351y | *Mol. Pharmaceutics* 2012, 9, 269−280

3.2. Preparation of Nanomicrosphere Carriers. Plain and curcumin-loaded PLGA nanoparticles were prepared using the "single emulsion−solvent evaporation" technique.[37] This preparation method is appropriate for the loading of hydrophobic cargos such as curcumin. Incorporation of the water-insoluble curcumin into polymeric nanoparticles would also improve its dissolution and accordingly its bioavailability. This advantageous role of the incorporation of curcumin in PLGA nanoparticles is shown in Scheme 2. From the scheme, the curcumin solubility in water was very limited (about 0.4 mg/mL at 25 °C, Scheme 2a). Scheme 2b illustrates the aqueous suspension of the curcumin-loaded PLGA nanoparticles. As can be noted, the incorporation of curcumin in PLGA nanoparticles formed a stable colloidal dispersion (4 mg/mL) with strong color, indicating a homogeneous distribution of curcumin in the aqueous medium. This enhancement in curcumin dissolution/distribution in water would consequently enhance the magnitude of curcumin absorption and bioavailability.

Scheme 2. A Schematic Illustration for Preparation of the Hydrogel Microspheres Encapsulating PLGA Nanoparticles as Carriers for Inhalation Therapy

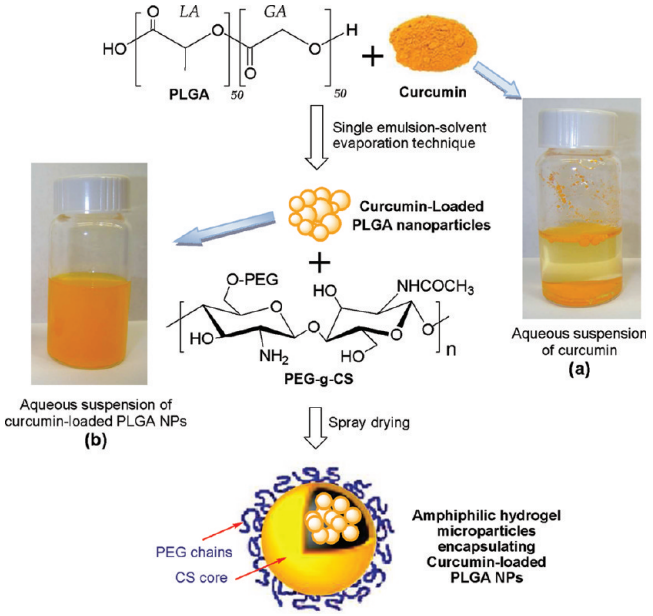

The curcumin-loaded PLGA nanoparticles were then incorporated into respirable/swellable microspheres. These microspheres were developed via spray drying of a homogeneous aqueous mixture of the curcumin-loaded PLGA nanoparticles with either CS or PEG-*g*-CS copolymer (Scheme 2). In the aqueous mixture of the PLGA nanoparticles and the PEG-*g*-CS copolymer, the hydrophilic PEG side chains are expected to be oriented outside toward water whereas the hydrophobic CS chains would be inside. Then, upon spray drying, the PEG and CS are expected to form the shell and core of the swellable particles, respectively, as illustrated in Scheme 2. The resulting series of nano−micro matrices (Table 1) were evaluated as carriers for sustained pulmonary drug delivery that combined the benefits of both nanoparticles and the swellable hydrogel microspheres suggested in our previous studies.[17,18]

3.3. Particle Size. The radius (R) of the prepared plain and curcumin-loaded PLGA nanoparticles was found to be 221.9 ± 16.6 and 243.4 ± 34.8 nm, respectively, as determined by DLS as shown in Figure 3a. In the case of the developed hydrogel microspheres, VMD was determined which represents the average diameter of the particles, and it provides a suitable estimation of particle size for dry powder inhalation purposes. From the size results shown in Table 1, the VMD values of the prepared curcumin-free and curcumin-loaded microspheres fall in the ranges of 3.11 ± 0.02 to 3.91 ± 0.10 and 3.08 ± 0.04 to 3.94 ± 0.01 μm, respectively. From the VMD data, it seems that increasing the PLGA content (%) in both plain and curcumin-loaded microspheres increases the particle size. However, this effect of PLGA % on particle size was found to be statistically insignificant. Also, both aerosolization performance and lung deposition efficiencies were assessed by determination of the aerodynamic diameters (d_a) of the particles with the aid of particle densities as described earlier in eq 3. As shown in Table 1, the developed microspheres attained relatively low tapped densities (in the range of 0.137−0.192 and 0.098−0.209 g/mL for curcumin-free and curcumin-loaded particles, respectively). From the density data and according to eq 3, the aerodynamic diameters (d_a) of the developed microspheres are likely to be significantly less than their geometric diameters (VMD) and fall in the range of 1.34 ± 0.01 to 1.64 ± 0.04 and 1.09 ± 0.02 to 1.80 ± 0.01 μm for curcumin-free and curcumin-loaded particles, respectively.

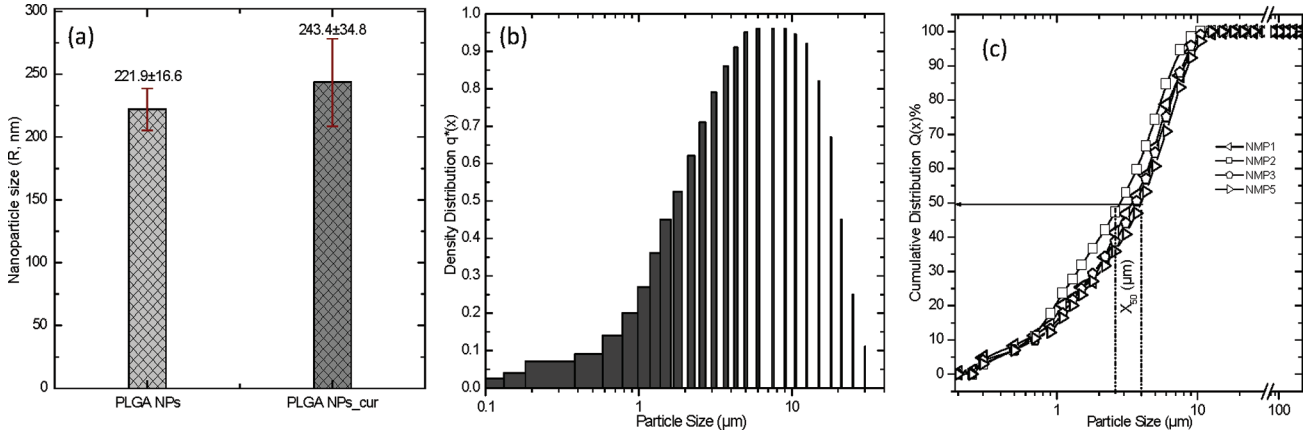

Figure 3. (a) The size (R, nm) of the prepared plain and curcumin-loaded PLGA nanoparticles as determined by DLS, (b) cumulative size distributions, and (c) density distributions of the developed hydrogel microspheres.

dx.doi.org/10.1021/mp200351y | *Mol. Pharmaceutics* 2012, 9, 269−280

These low values of d_a explain the relatively high respirability (high R_F values) of the prepared carrier systems as will be shown in the aerosol dispersion study (section 3.9). Both cumulative size and density distributions of the prepared curcumin-loaded particles are illustrated in Figure 3b,c. These figures confirmed that the average particle size is about 2.5−4 μm. The mass median aerodynamic diameters (MMAD) of the prepared microspheres were also estimated and found to be in the range of 1.25−1.96 μm.

3.4. Surface Morphology Study. Figure 4 shows the scanning electron micrographs of some of the developed hydrogel microspheres encapsulating curcumin-loaded PLGA nanoparticles. As apparent from the figure, the prepared hydrogel particles have a spherical nature with highly smooth and integrated surfaces. Also, the microspheres showed relatively porous surfaces. This porous nature may be attributed to the rapid evaporation of any residual solvents such as ethanol and/or methylene chloride from the PLGA/polymer mixture during the spray drying process. Figure 4b illustrates some collapsed hydrogel microspheres encapsulating inside themselves some curcumin-loaded PLGA nanoparticles.

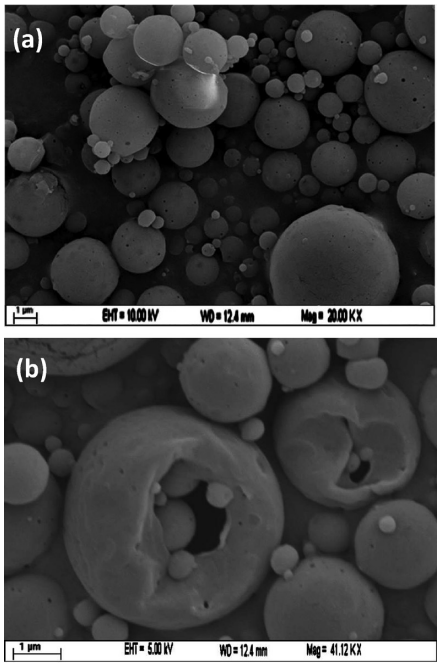

Figure 4. Scanning electron micrographs of some developed hydrogel microspheres encapsulating curcumin-loaded PLGA nanoparticles.

3.5. Moisture Content. The moisture content (%) of the plain and curcumin-loaded hydrogel microspheres developed in this study is illustrated in Table 1. As apparent from the data, the moisture content (%) falls in the ranges of (0.90 ± 0.31 to 1.46 ± 0.06) and (1.21 ± 0.10 to 1.76 ± 0.14) for plain and curcumin-loaded microspheres, respectively. As apparent from the moisture content data (Table 1), the developed particles showed relatively low percents of moisture. These low moisture percentages are significant for avoiding drug degradation and attaining long-term stability. Also, the low moisture contents decrease the particle density and accordingly enhance the aerodynamic performance of the particles through the inhalation process.

3.6. Dynamic Swelling Study. The swelling patterns of the hydrogel microspheres encapsulating curcumin-loaded PLGA nanoparticles in PBS, pH 7.4 are illustrated in Figure 5. As apparent in the figure, the swelling profiles of the particles were obtained by determining the increase in both median diameters (X_{50}, μm) and the volume mean diameter (VMD, μm) of the particles at different time intervals with the aid of laser diffraction. As shown in Figure 5, most of the prepared formulations showed a fast initial swelling within the first few minutes. For example, the VMD of NMP1, NMP2 and NMP3 particles has increased from about 3−3.5 μm when dry to 38.1, 32.4, and 30.2 μm, respectively, after 6 min of swelling. This swelling continues regularly with time to reach 91.0, 82.8, and 82.7 μm at 20 min, respectively. It can be noted also from the figure that the formulations based on the PEG-*g*-Cs attained higher swelling values as compared to the formulations based

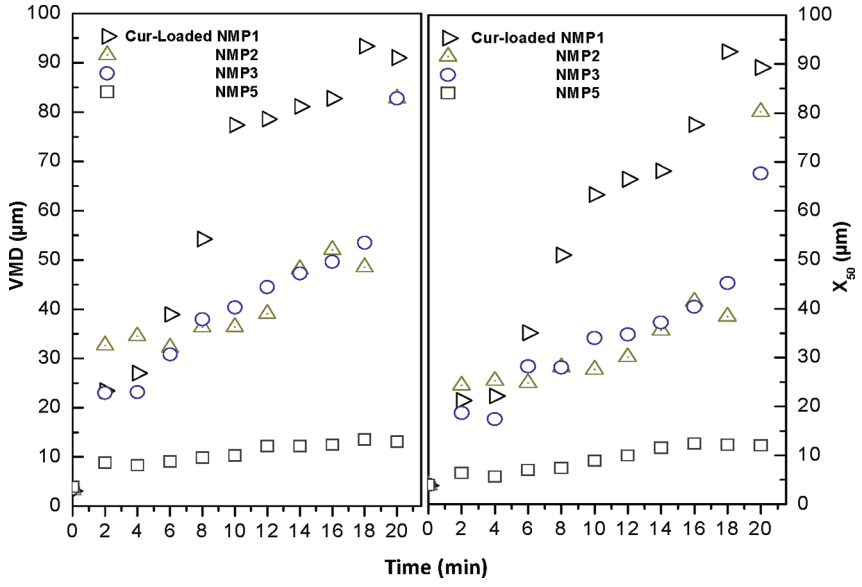

Figure 5. Dynamic swelling profiles of the developed curcumin-loaded hydrogel particles, expressed as volume mean diameter (VMD, μm) and median diameter (X_{50}, μm) in PBS, pH 7.4.

on Cs (NMP5). This can be attributed to the hydrophilicity of the PEG side chains in the PEG-*g*-Cs copolymer. Also, from Figure 5, it seems that increasing the PLGA content in the microspheres through moving from NMP1 (35% PLGA) to NMP2 (50% PLGA) and NMP3 (75% PLGA) tends to decrease the swelled sizes of the hydrogel particles. This behavior may be due to the hydrophobic nature of the PLGA which may retard the entrance of the aqueous swelling fluid to the particle matrices.

3.7. *In Vitro* Biodegradation Study. The biodegradation study of the curcumin-loaded hydrogel matrices was performed in PBS, pH 7.4 in presence of 2 mg/mL of lysozyme.[38] Lysozyme, a 14 kDa cationic protein consisting of a single polypeptide chain, was used due to it is high abundance (as antimicrobial polypeptide) in respiratory tract secretions.[39] Lysozyme is also secreted onto epithelial surfaces and was found in the primary and secondary granules of neutrophils, as well as the granules of mononuclear phagocytes.[39] The percentage of weight remaining of the particles was determined as a function of time and taken as a measure of degradation. The enzymatic degradation patterns of the investigated curcumin-loaded particles are illustrated in Figure 6. As

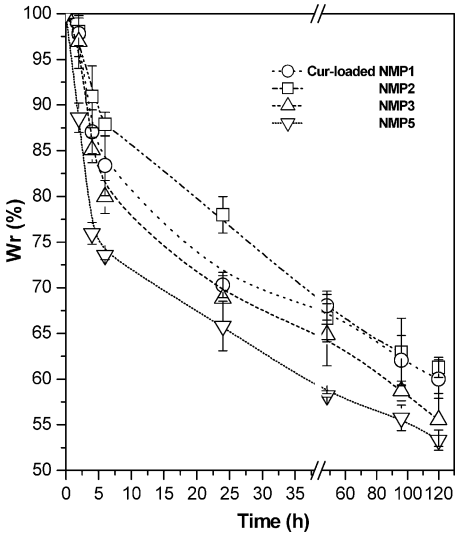

Figure 6. *In vitro* enzymatic degradation extents of the prepared curcumin-loaded hydrogel particles as investigated in PBS, pH 7.4 at 37 °C.

apparent from the figure, enzymatic degradation of the hydrogel particles was starting to occur within the first few hours. It is apparent also that the hydrogel matrices based on CS (NMP5) showed relatively more enzymatic degradation as compared to the formulations based on PEG-*g*-CS. The reduction in the degradation of the copolymer-based formulations relative to the CS-based one can be attributed to presence of the PEG, which known by its low biodegradability. Moreover, it seems that decreasing the percent of the biodegradable PLGA in the particles tends to decrease the degradation extent (high remaining weights). For instance, at 120 h, the remaining weights of NMP3 (75% PLGA), NMP2 (50% PLGA) and NMP1 (35% PLGA) were 55.5 ± 2.9, 60.0 ± 2.1 and 61.3 ± 1.1, respectively. However, this effect of PLGA % was found to be statistically insignificant.

3.8. *In Vitro* Cumulative Release Studies. The entrapment efficiencies (EE %) of curcumin in the prepared formulations were determined with the aid of UV−vis spectrophotometry. The data shown in Table 1 reveals that the EE % values of the loaded curcumin fall in the range of 89.63 ± 1.28 to 94.42 ± 1.71. Also, from the data, it seems that the particle composition has a nonsignificant effect on the EE% values.

The release profiles of curcumin from NMP2, NMP3 and NMP5 formulations, as examples, are illustrated in Figure 7.

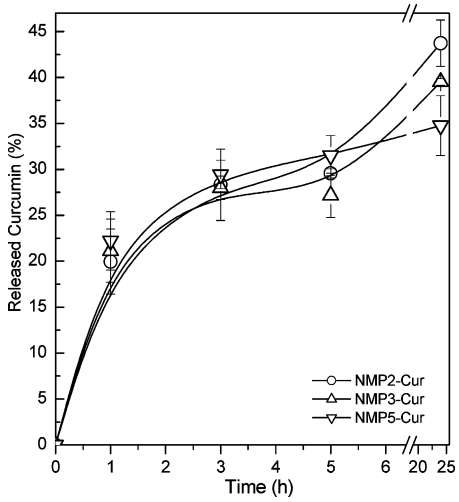

Figure 7. Cumulative release profiles of curcumin from some of the developed hydrogel microspheres encapsulating PLGA nanoparticles in PBS, pH 7.4 at 37 °C.

From the figure, the three investigated formulations showed a fast initial release of curcumin (about 20%) within the first hour followed by a relatively slow release. The burst release may be attributed to the fast initial dynamic swelling of the particles (see section 3.6) as the principal mechanism that explains such release is based on the diffusion through the swollen hydrogel particles. Also, from the figure, it seems that the curcumin (%) released from the particles based on the PEG-*g*-Cs copolymer is relatively higher than that released from Cs-based particles. For example, at 24 h, the curcumin % released from NMP2 and NMP5 was 43.1 ± 4.8 and 33.9 ± 5.2, respectively. However, the difference was found statistically nonsignificant. Also, it seems that increasing the PLGA content within the developed hydrogel particles tends to decrease the amount of curcumin released. For instance, the curcumin percentages released at 24 h from NMP2 (50% PLGA) and NMP3 (75% PLGA) were 43.1 ± 4.8 and 39.6 ± 1.4, respectively. These release results are in agreement with the swelling patterns discussed earlier in section 3.6.

3.9. *In Vitro* Aerosolization Study. The powder aerosolization characteristics of the curcumin-loaded NMP1 formulation, as an example, were assessed *in vitro* using a dry-powder, breath-activated inhaler device (Handihaler DPI) with the aid of an NGI at air flow rate of 60 ± 5% L/min. The drug deposition (%) on each stage of the NGI, preseparator, adapter, inhaler device and the capsule was estimated and plotted as illustrated in Figure 8. This stage by stage deposition data shown in the figure demonstrates that, indeed, the hydrogel particles are able to be dispersed as a dry powder without issue. Also from the data in Figure 8 and with the aid of eq 4, the average emitted fraction, E_F%, of the curcumin-loaded NMP1 powder was determined to be 98.1%. The average respirable

dx.doi.org/10.1021/mp200351y | *Mol. Pharmaceutics* 2012, 9, 269−280

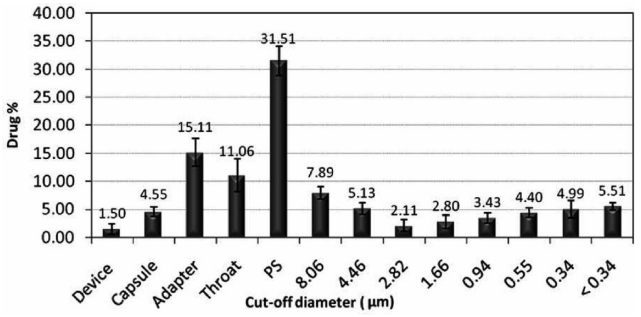

Figure 8. *In vitro* dry powder aerosolization study using NGI at a flow rate of 60 L/min and using a Handihaler as inhaler device (PS: the preseparator of the NGI).

fraction, R_F%, of the investigated hydrogel powder (NMP1-cur) was found to be 28.4 ± 6.0%, and the fine particle fraction, FP_F % (cutoff diameters, d_a < 4.46 μm), was found to be 30.2 ± 6.5%. The FP_F is the fraction of dry powder that would likely deposit in the deep lung. The obtained FP_F % value is promising and matches most of the dry powder inhaler systems currently available in the market. Further formulation optimization of the developed aerosol hydrogel particles through interactive combination with lactose as a standard excipient with most DPIs will need to be performed and can further improve the aerosol dispersion performance.

3.10. Cytotoxicity Assay. The viability of Raw 264.7 macrophage cells was estimated after exposure of the cells for 24 h to different plain and curcumin-loaded swellable microparticles formulations at different concentrations as apparent in Figure 9. From Figure 9a, at a concentration of 800 μg/mL, the viability of the cells was not affected by the curcumin-free microparticles irrespective the composition (NMP2, NMP3, and NMP5) and resulted in practically no toxicity. However, both curcumin-loaded PLGA and NMP3 microparticles have significantly (p < 0.05) reduced the Raw 264.7 cell viability (by 85.1% and 57.9%, respectively), under the same experimental conditions. Also, as noted from the figure, the tested curcumin-loaded NMP3 microparticles affected the cells relatively less than the curcumin-loaded PLGA particles under the same conditions. This behavior may be attributed to the increase of local acidity caused by the degradation of PLGA particles, which led to more cell damage, as suggested in some previous studies.[42,43]

The effect of particle concentration on the viability of Raw 264.7 macrophage cells was also determined by the MTT assay after exposure of the cells for 24 h to different concentrations (320, 800, and 1600 μg/mL) of NMP2 and NMP5 particles suspensions (Figure 9b). From the figure, within the investigated range of concentrations, the viability of the cells was not affected by microparticles irrespective of their concentration and resulted in no statistical differences in cell viability (p < 0.05). These results reveal a low cytotoxic potential for the developed swellable particle drug delivery systems.

3.11. TNF-α Assay. Figure 10 shows the TNF-α values as quantified in the RAW 264.7 cells incubated with the developed plain and curcumin-loaded swellable particles in addition to negative controls (PS 1 μm and PS 112 μm). As apparent from the figure, the cells stimulated with 1600 μg mL^{-1} of the NMP3 microparticles have secreted significantly (p < 0.05) higher levels of TNF-α compared to the cell-only negative control and the cells containing the same concentration of other plain and

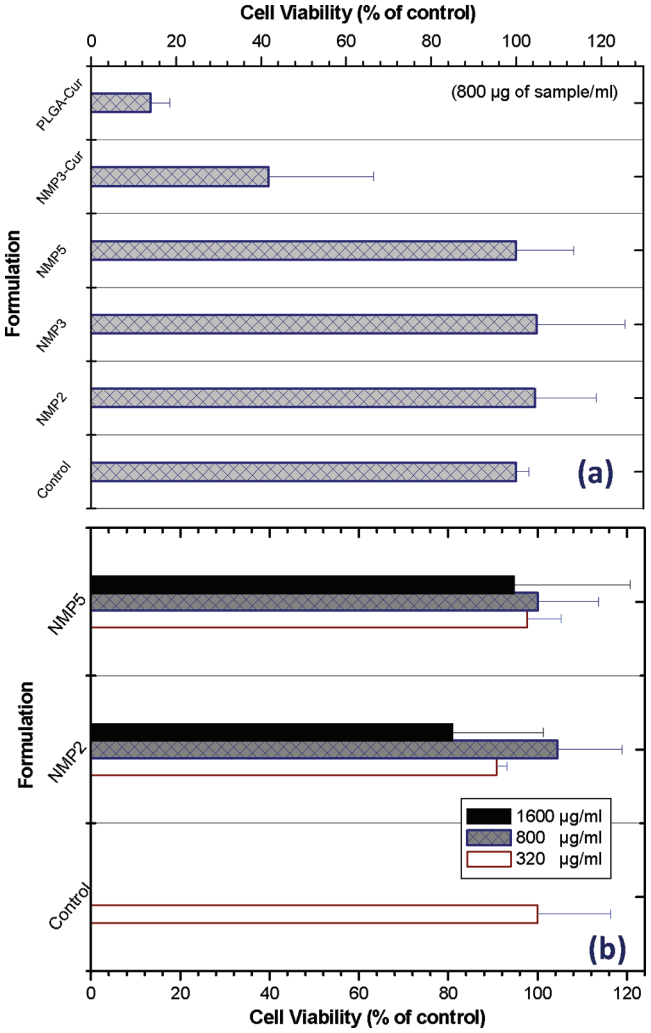

Figure 9. Viability (% of control) of Raw 264.7 macrophage cells after they have been incubated for 24 h with (a) some of the developed plain and curcumin-loaded swellable microparticles formulations (800 μg/mL), and (b) various concentrations (320, 800, and 1600 μg/mL). Cell viability was measured by the MTT assay, as explained in detail in section 3.10. The data represents the mean value of three trials ± SD.

curcumin-loaded microparticles. Also, it seems from the figure that the cells exposed to curcumin-loaded particle formulations have secreted almost similar amounts of TNF-α as those exposed to free curcumin. This preliminary data tends to demonstrate that the swellable microparticles developed in this study have minimal propensity to induce TNF-α release and therefore may not induce a local inflammatory response.

3.12. Macrophage Uptake Study. The major obstacle against the development of sustained pulmonary drug delivery formulations is that the most appropriate aerodynamic size for particles to be respirable (0.5−5 μm) is also the optimum size for the rapid uptake by the macrophages in the alveolar region. This leads to a rapid phagocytosis of carrier particles and loss of the entrapped therapeutic molecules. Microparticles of this size are rapidly engulfed and phagocytosed by macrophages in the airways on the order of minutes as was noted with the nonswellable fluorescent 1 μm polystyrene particles, PS-1 (Figure 11). In contrast, the swollen hydrogel nano−microparticles, developed in this study (NMP2, NMP5, and PLGA-cur as examples), showed much delayed and reduced macrophage uptake (Figures 11and 12b−d). This reduced

dx.doi.org/10.1021/mp200351y | *Mol. Pharmaceutics* 2012, 9, 269−280

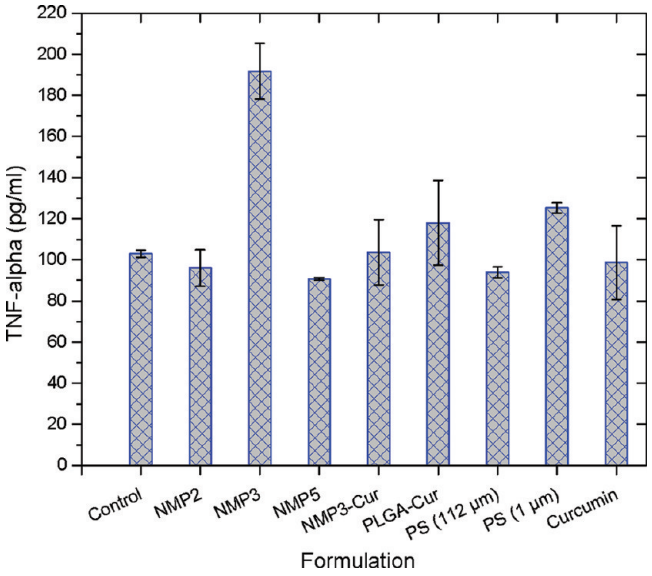

Figure 10. The TNF-α values as quantified in the RAW 264.7 macrophage cells containing (1600 μg/mL) of some of the prepared plain, curcumin-loaded swellable particles, and control particles (PS 1 μm and PS 112 μm) compared to the cell-only negative control. The results are presented as the mean TNF-α that corresponds the Abs_{450} minus Abs_{550}) with 95% confidence limits. The data represents the mean value of three trials ± SD.

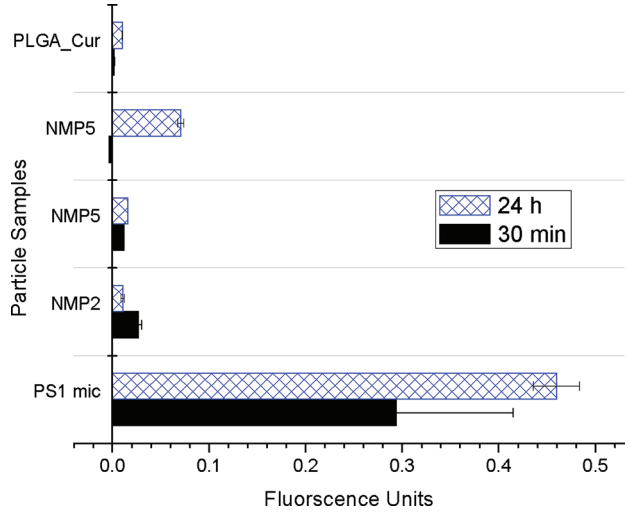

Figure 11. Phagocytic uptake efficiency of some of the developed swellable nano–microparticles in as compared to control particles (nonswellable 1 μm PS), at two time points (30 min and 24 h), as quantified by measuring the absorbance at 430 nm corresponding to the retained/uptaken fluorescent particles after washing the excess particles [L, 4 mg/mL; and H, 7 mg/mL].

phagocytosis can be ascribed to the rapid and high swelling attained by the developed microparticles as compared to the PS-1 control particles up to 24 h of incubation with the macrophage cells (Figure 11). In addition, the PEG in the PEG-*g*-Cs copolymer used to develop the swellable microparticles can play a significant role in enhancing stealth characteristics of the particles to evade the macrophage uptake. These *in vitro* macrophage interaction studies illustrated that the swellable nano–microparticle systems developed in this study may have the potential for sustained pulmonary drug delivery. Current *in vivo* studies are also underway to investigate the suitability of

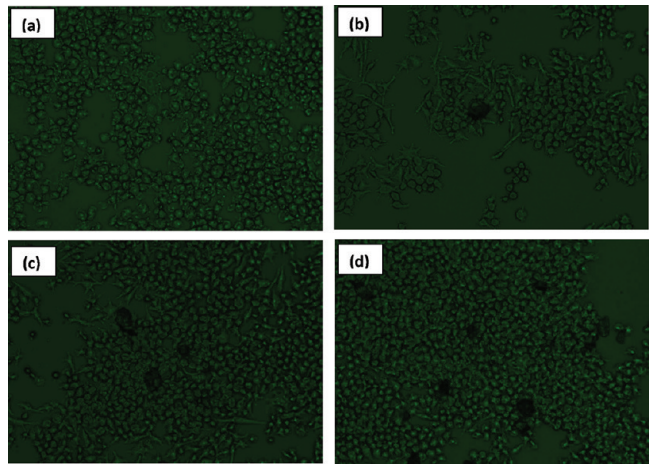

Figure 12. *In vitro* particle uptake by macrophages at 24 h incubation time point (a) control cells, and swellable (b) NMP2, (c) NMP5, and (d) PLGA-Cur microparticles. The imaging of retained microparticles was determined at low magnification (20×).

the developed particles as potential carriers for the controlled drug release in the lungs.

4. CONCLUSION

In this study, PLGA nanoparticles encapsulated in amphiphilic PEG-Cs copolymer-based hydrogel microspheres were developed and evaluated as a new potential carrier system for sustained pulmonary delivery of curcumin using DPIs. This carrier system merges the advantages of nanoparticles and the respirable/swellable hydrogel microspheres proposed earlier by our group while avoiding their shortcomings. The *in vitro* assessment showed a potential of the nano–micro particles developed in this study as potential carriers for sustained pulmonary delivery of curcumin.

AUTHOR INFORMATION

Corresponding Author

*University of Texas at Austin, College of Pharmacy, 1 University Station, Austin, Texas 78712. Tel: +1 (512) 471-3383; Fax: +1 (512) 471-7474. E-mail: hsmyth@mail.utexas.edu.

ACKNOWLEDGMENTS

This research was supported by National Institutes of Health, National Institute of Biomedical Imaging and Bioengineering (REB006892A), Oxnard Foundation, PhRMA Foundation and CF Foundation.

REFERENCES

(1) Patton, J. S.; Byron, P. R. Inhaling medicines: delivering drugs to the body through the lungs. *Nat. Rev. Drug Discovery* **2007**, *6*, 67–74.
(2) Lu, D.; Hickey, A. J. Pulmonary vaccine delivery. *Expert Rev. Vaccines* **2007**, *6*, 213–226.
(3) Hickey, A. J. Inhalation aerosols: physical and biological basis for therapy; Marcel Dekker: New York, 1996.
(4) Laube, B. L. The expanding role of aerosols in systemic drug delivery, gene therapy, and vaccination. *Respir. Care.* **2005**, *50*, 1161–1176.
(5) Wu, L.; da Rocha, S. R. P. Biocompatible and biodegradable copolymer stabilizers for hydrofluoroalkane dispersions: a colloidal probe microscopy investigation. *Langmuir* **2007**, *23*, 12104–12110.

(6) Suh, J.; Choy, K. L.; Lai, S. K.; Suk, J. S.; Tang, B. C.; Prabhu, S.; Hanes, J. PEGylation of nanoparticles improves their cytoplasmic transport. *Int. J. Nanomed.* **2007**, *2*, 735−741.
(7) Wu, L.; Al-Haydari, M.; da Rocha, S. R. Novel propellant-driven inhalation formulations: engineering polar drug particles with surface-trapped hydrofluoroalkane-philes. *Eur. J. Pharm. Sci.* **2008**, *33*, 146−158.
(8) Shoyele, S. A.; Cawthorne, S. Particle engineering techniques for inhaled biopharmaceuticals. *Adv. Drug Delivery Rev.* **2006**, *58*, 1009−1029.
(9) Patton, J. S.; Bukar, J.; Nagarajan, S. Inhaled insulin. *Adv. Drug Delivery Rev.* **1999**, *35*, 235−247.
(10) Wang, Y. Y.; Lai, S. K.; Suk, J. S.; Pace, A.; Cone, R.; Hanes, J. Addressing the PEG mucoadhesivity paradox to engineer nanoparticles that "slip" through the human mucus barrier. *Angew. Chem., Int. Ed.* **2008**, *47*, 9726−9729.
(11) Grenha, A.; Seijo, B.; Remuñán-López, C. Microencapsulated chitosan nanoparticles for lung protein delivery. *Eur. J. Pharm. Sci.* **2005**, *25*, 427−437.
(12) Dickinson, P. A.; Howells, S. W.; Kellaway, I. W. Novel nanoparticles for pulmonary drug administration. *J. Drug Targeting* **2001**, *9*, 295−302.
(13) Dellamary, L. A.; Tarara, T. E.; Smith, D. J.; Woelk, C. H.; Adractas, A.; Costello, M. L.; Gill, H.; Weers, J. G. Hollow porous particles in metered dose inhalers. *Pharm. Res.* **2000**, *17*, 168−174.
(14) Edwards, D. A.; Hanes, J.; Caponetti, G.; Hrkach, J.; Ben-Jebria, A.; Eskew, M. L.; Mintzes, J.; Deaver, D.; Lotan, N.; Langer, R. Large porous particles for pulmonary drug delivery. *Science* **1997**, *276*, 1868−1872.
(15) Yang, Y.; Bajaj, N.; Xua, P.; Ohnd, K.; Tsifanskye, M. D.; Yeo, Y. Development of highly porous large PLGA microparticles for pulmonary drug delivery. *Biomaterials* **2009**, *30*, 1947−1953.
(16) Koushik, K.; Dhanda, D.; Cheruvu, N.; Kompella, U. Pulmonary delivery of deslorelin: large-porous PLGA particles and HPβCD complexes. *Pharm. Res.* **2004**, *21*, 1119−1126.
(17) El-Sherbiny, I. M.; Smyth, H. D. C. Biodegradable nano-micro carrier systems for sustained pulmonary drug delivery: (I) self-assembled nanoparticles encapsulated in respirable/swellable semi-IPN microspheres. *Int. J. Pharm.* **2010**, *395*, 132−141.
(18) El-Sherbiny, I. M.; McGill, S.; Smyth, H. D. C. Swellable microparticles as carriers for sustained pulmonary drug delivery. *J. Pharm. Sci.* **2010**, *99*, 2343−2356.
(19) El-Sherbiny, I. M.; Smyth, H. D. C. Novel cryomilled physically crosslinked biodegradable hydrogel microparticles as carriers for inhalation therapy. *J. Microencapsul.* **2010**, *27*, 657−668.
(20) Ammon, H. P. T; Wahl, M. A. Pharmacology of curcuma longa. *Planta Med.* **1991**, *57*, 1−7.
(21) Cheng, A. L.; Hsu, C. H.; Lin, J. K.; Hsu, N. M.; Ho, Y. F.; Shen, T. S.; Ko, J. Y.; Lin, J. T.; Lin, B. R.; Ming-Shiang, W.; Yu, H. S.; Jee, S. H.; Chen, G. S.; Chen, T. M.; Chen, C. A.; Lai, M. K.; Pu, Y. S.; Pan, M. H.; Wang, Y. J.; Tsai, C. C.; Hsieh, C. Y. Phase I clinical trial of curcumin, a chemopreventive agent, in patients with high-risk or pre-malignant lesions. *Anticancer Res.* **2001**, *21*, 2895−2900.
(22) Mukhopadhyay, A.; Basu, N.; Ghatak, N.; Gujral, P. K. Antiinflammatory and irritant activities of curcumin analogues in rats. *Agents Actions* **1982**, *12*, 508−515.
(23) Reddy, A. C.; Lokesh, B. R. Effect of dietary turmeric (Curcuma longa) on iron induced lipid peroxidation in the rat liver. *Food Chem. Toxicol.* **1994**, *32*, 279−283.
(24) Huang, M.; Newmark, H. L.; Frenkel, K. Inhibitory effects of curcumin on tumorigenesis in mice. *J. Cell Biochem.* **1997**, *67*, 26−34.
(25) Egan, M. E.; Pearson, M.; Weiner, S. A.; Rajendran, V.; Rubin, D.; Glöckner-Pagel, J.; Canny, S.; Du, K.; Lukacs, G. L.; Caplan, M. J. Curcumin, a major constituent of turmeric, corrects cystic fibrosis defects. *Science* **2004**, *304*, 600−602.
(26) Sethi, G.; Sung, B.; Aggarwal, B. B. The role of curcumin in modern medicine. *Herbal Drugs: Ethnomedicine to Modern Medicine*; Ramawat, K. G., Ed.; Springer-Verlag: Berlin, Heidelberg, 2009; Chapter 7, pp 97−113.
(27) Dhillon, N.; Aggarwal, B. B.; Newman, R. A.; Wolff, R. A.; Kunnumakkara, A. B.; Abbruzzese, J. L.; Ng, C. S.; Badmaev, V.; Kurzrock, R. Phase II Trial of curcumin in patients with advanced pancreatic cancer. *Clin. Cancer Res.* **2008**, *14*, 4491−4499.
(28) Selvam, P.; El-Sherbiny, I. M.; Smyth, H. D. Swellable hydrogel particles for controlled release pulmonary administration using propellant-driven metered dose inhalers. *J. Aerosol Med. Pulm. Drug Delivery* **2011**, *24*, 25−34.
(29) Oberdorster, G. Pulmonary effects of inhaled ultrafine particles. *Int. Arch. Occup. Environ. Health* **2001**, *74*, 1−8.
(30) Krenis, L. J.; Strauss, B. Effect of size and concentration of latex particles on respiration of human blood leucocytes. *Proc. Soc. Exp. Biol.* **1961**, *107*, 748−750.
(31) Kawaguchi, H.; Koiwai, N.; Ohtsuka, Y.; Miyamoto, M.; Sasakawa, S. Phagocytosis of latex particles by leukocytes. I. Dependence of phagocytosis on the size and surface potential of particles. *Biomaterials* **1986**, *7*, 61−66.
(32) Rudt, S.; Muller, R. H. In vitro phagocytosis assay of nano- and microparticles by chemiluminescence. I. Effect of analytical parameters, particle size and particle concentration. *J. Controlled Release* **1992**, *22*, 263−271.
(33) Heyder, J.; Rudolf, G. Mathematical models of particle deposition in the human respiratory tract. *J. Aerosol Sci.* **1984**, *15*, 697−707.
(34) Astete, C. E.; Sabliov, C. M. Synthesis and characterization of PLGA nanoparticles. *J. Biomater. Sci., Polym. Ed.* **2006**, *17*, 247−289.
(35) Majeti, N. V.; Kumar, R. A review of chitin and chitosan applications. *React. Funct. Polym.* **2000**, *46*, 1−27.
(36) Parka, J. H.; Kwon, S.; Lee, M.; Chung, H.; Kim, J. H.; Kim, Y. S.; Park, R. W.; Kim, I. S.; Seo, S. B.; Kwon, I. C.; Jeong, S. Y. Self-assembled nanoparticles based on glycol chitosan bearing hydrophobic moieties as carriers for doxorubicin: In vivo biodistribution and anti-tumor activity. *Biomaterials* **2006**, *27*, 119−126.
(37) Cartiera, M. S.; Ferreira, E. C.; Caputo, C.; Egan, M. E.; Caplan, M. J.; Saltzman, M. Partial correction of cystic fibrosis defects with PLGA nanoparticles encapsulating curcumin. *Mol. Pharmaceutics* **2010**, *7*, 86−93.
(38) Hirano, S.; Tsuchida, H.; Nagao, N. N-Acetylation in chitosan and the rate of its enzymic hydrolysis. *Biomaterials* **1989**, *10*, 574−6.
(39) Ganz, T Antimicrobial polypeptides in host defense of the respiratory tract. *J. Clin. Invest.* **2002**, *109*, 693−697.
(40) Guinesi, L. S.; Cavalheiro, E. T. G. The use of DSC curves to determine the acetylation degree of chitin/chitosan samples. *Thermochim. Acta* **2006**, *444*, 128−133.
(41) Kittur, F. S.; Prashanth, K. V. H.; Sankar, K. U.; Tharanthan, R. N. Characterization of chitin, chitosan and their carboxymethyl derivatives by differential scanning calorimetry. *Carbohydr. Polym.* **2002**, *49*, 185−193.
(42) Murillo, M.; Gamazo, C.; Goni, M. M.; Irache, J. M.; Blanco-Príeto, M. J. Development of microparticles prepared by spray-drying as a vaccine delivery system against brucellosis. *Int. J. Pharm.* **2002**, *242*, 341−344.
(43) Pillai, O.; Panchagnula, R. Polymers in drug delivery. *Curr. Opin. Chem. Biol.* **2001**, *5*, 447−451.